SHORT-RANGE ORDER-DISORDER IN GEM RICHTERITE AND PARGASITE FROM AFGHANISTAN: CRYSTAL-STRUCTURE REFINEMENT AND INFRARED SPECTROSCOPY

Maxwell C. DAY AND Frank C. HAWTHORNE[§]

Department of Geological Sciences, University of Manitoba, Winnipeg, Manitoba R3T 2N2, Canada

Umberto SUSTA AND Giancarlo DELLA VENTURA

Dipartimento di Scienze, Università di Roma Tre, Largo San Leonardo Murialdo 1, 00146 Rome, Italy

George E. HARLOW

Department of Earth and Planetary Sciences, American Museum of Natural History, Central Park West at 79th Street, New York, New York 10024-5192, U.S.A.

ABSTRACT

The crystal structures of gem-quality richterite and pargasite from Afghanistan, space group $C2/m$, $Z = 2$, have been refined to R_1 indices of 2.47% and 3.22%, respectively, using Mo$K\alpha$ X-radiation. Results from electron-microprobe analysis were used to calculate unit formulae and site populations were assigned using the refined site-scattering values and the observed mean bond-lengths. In pargasite, $^{[4]}$Al is strongly ordered at $T(1)$ and $^{[6]}$Al is partly disordered over the $M(2)$ and $M(3)$ sites, whereas the $M(1,2,3)$ sites are almost completely occupied by Mg in richterite. ^{A}Na is split between the $A(2)$ and $A(m)$ sites and K occurs at the $A(m)$ site. The infrared spectra in the principal OH-stretching region were measured and the fine structure was fit to component bands that were assigned to short-range ion arrangements over the configuration symbol $M(1)M(1)M(3)$–O(3)–A–O(3):$T(1)T(1)$, corresponding to the following local arrangements: MgMgMg–OH–Na–OH:SiSi; MgMgMg–OH–Na–F:SiSi; MgMgMg–OH–Na–F:SiAl; and MgMgMg–OH–□–OH:SiSi in richterite and MgMgMg–OH–Na–OH:SiAl; MgMgMg–OH–Na–F:SiAl; MgMgAl–OH–Na–OH:SiAl; and MgMgAl–OH–Na–F:SiAl in pargasite (□ = vacancy).

Keywords: pargasite, richterite, amphibole, gem, crystal structure, infrared spectroscopy, Afghanistan, short-range order.

INTRODUCTION

There has been considerable work done on short-range arrangements in amphiboles, focusing primarily on synthetic amphiboles (Raudsepp *et al.* 1987a, b, Robert *et al.* 1989, Della Ventura *et al.* 1996a, b, 1997, 1998a, b, 1999, 2001, 2003, Hawthorne *et al.* 1997, 2000, Robert *et al.* 1999, Najorka & Gottschalk 2003) and gem amphiboles (Tait *et al.* 2001, Abdu & Hawthorne 2009, Heavysege *et al.* 2015, Day *et al.* 2018), as rock-forming amphiboles are commonly too complicated from a chemical perspective to allow derivation of all short-range arrangements of their

constituent ions. Although we know that the occurrence of short-range arrangements in amphiboles is driven primarily by local bond-valence requirements of the constituent ions (Hawthorne 1997), what is not clear is whether conditions of crystallization or equilibration affect such short-range arrangements (in much the same way as conditions of crystallization affect the chemical composition of a mineral). Thus it is important to derive local atomic arrangements in both amphiboles from different localities and also across a wide range of amphibole compositions such that a coherent picture of short-range behavior can be built up. Here, we compare local atomic arrangements

[§] *Corresponding author e-mail address*: frank_hawthorne@umanitoba.ca

TABLE 1. UNIT-CELL DIMENSIONS AND CRYSTALLOGRAPHIC DATA FROM STRUCTURE REFINEMENTS FOR GEM AMPHIBOLES FROM AFGHANISTAN

	AM4	AM5
a (Å)	9.845(5)	9.885(6)
b	17.940(10)	17.978(12)
c	5.294(3)	5.283(4)
β (°)	105.221(7)	105.193(7)
V (Å³)	902.2(9)	906.0(2)
Crystal size (μm)	$10 \times 50 \times 110$	$60 \times 90 \times 100$
Crystal color	clear	clear
Radiation/ monochronometer	Mo$K\alpha$	Mo$K\alpha$
Total reflections	16448	16258
Reflections in Ewald sphere	5324	5310
Unique reflections	1379	1376
R_1 %	2.53	3.22
R(int) %	1.26	1.19
wR %	7.22	7.57
GoF	0.878	0.863
Z	2	2

in gem-quality richterite (AM4) and pargasite (AM5) from Afghanistan by single-crystal structure refinement, infrared spectroscopy, and electron-microprobe analysis and compare the results for pargasite from several localities.

EXPERIMENTAL

Single-crystal structure refinement (SREF), electron microprobe analysis (EMPA), and Fourier-transform infrared spectroscopy (FTIR) were done at the Department of Geological Sciences, University of Manitoba. Crystals were selected based on clarity and uniform extinction under cross-polarized light. In preparation for SREF, samples were attached to tapered glass fibers; similar samples were double-polished for FTIR analysis. For EMPA, samples were mounted in epoxy in an acrylic ring, ground, polished, and carbon coated.

X-ray diffraction (SREF)

Single-crystal X-ray analysis was done using a Bruker D8 three-circle diffractometer equipped with a rotating-anode generator producing monochromatic Mo$K\alpha$ X-radiation, multilayer optics, and an APEX-II CCD detector. Totals of ~16,300 intensities were collected to 60° 2θ using 2–4 s per 0.2° frame with a crystal-to-detector distance of 5 cm. Empirical absorption corrections (SADABS, Sheldrick 2008) were applied. Equivalent reflections were merged, resulting in ~5320 reflections in the Ewald sphere, intensities were averaged for the space group $C2/m$ resulting in ~1377 unique reflections, and intensities were reduced to structure factors. Unit-cell dimensions were obtained by least-squares refinement of the positions of ~4000 reflections with $I > 10\sigma I$ and are given in Table 1. Each structure was refined in the space group $C2/m$ with the SHELXTL version 6.14 program (Bruker AXS) to average R indices of ~2.88% with anisotropic-displacement parameters at all sites. Atom positions and anisotropic-displacement parameters are given in Table 2. Selected interatomic distances are given in Table 3. Both .cif files may be obtained from The Depository of Unpublished Data on the MAC website [document gem richterite and pargasite, CM56, 18-00052][1].

Electron microprobe analysis (EMPA)

Chemical analyses were done with a Cameca SX-100 electron microprobe operated in wavelength-dispersive mode using a voltage of 15 kV, a beam current of 20 nA, and a beam size of 1 μm. The following standards were used for $K\alpha$ lines: Na, albite; Si, Ca, diopside; F, F-riebeckite; Mg, olivine; Al, andalusite; K, orthoclase; Ti, titanite; Fe, fayalite; Mn, Zn, V, Cr, and Cl were sought but not detected. Ten analytical points were measured on both samples. Data were corrected using the PAP procedure of Pouchou & Pichoir (1985), and the mean compositions are given in Table 4, together with the unit formulae calculated on the basis of (O,OH,F) = 24 atoms per formula unit (*apfu*) with (OH,F) = 2 *apfu*.

Infrared spectroscopy (FTIR)

Fourier-Transform InfraRed (FTIR) spectra in the principal (OH)-stretching region were collected using a Bruker Tensor 27 FTIR spectrometer equipped with a KBr beam splitter and a DLATGS detector. Spectra over the range 4000–400 cm⁻¹ were collected by averaging 100 scans at an operating resolution of 4 cm⁻¹ and base-line corrections were done using the OPUS spectroscopic software. Spectral analysis in the 3800–3600 cm⁻¹ range was done using the OMNIC software. Spectra were fit using Gaussian curves of similar width (full-width-at-half-maximum) with the program FITYK V0.9.8.

---

[1] The MAC website can be found at http://mineralogicalassociation.ca/

TABLE 2. ATOM COORDINATES AND ANISOTROPIC-DISPLACEMENT PARAMETERS (Å²) FOR GEM-QUALITY AMPHIBOLES FROM AFGHANISTAN

Site	x	y	z	U^{11}	U^{22}	U^{33}	U^{23}	U^{13}	U^{12}	$U^{eq/iso}$
					AM4					
T(1)	0.27764(4)	0.08494(2)	0.29725(8)	0.00620(18)	0.00615(19)	0.00631(19)	−0.00025(12)	0.00117(13)	−0.00034(11)	0.00632(13)
T(2)	0.28633(4)	0.17175(2)	0.80340(8)	0.00576(18)	0.00624(19)	0.00587(19)	−0.00037(12)	0.00136(13)	−0.00081(11)	0.00600(13)
M(1)	0	0.08904(4)	½	0.0078(3)	0.0076(3)	0.0065(3)	0	0.0019(2)	0	0.0074(3)
M(2)	0	0.17882(4)	0	0.0071(3)	0.0071(3)	0.0089(3)	0	0.0024(2)	0	0.0077(3)
M(3)	0	0	0	0.0078(4)	0.0063(4)	0.0065(4)	0	0.0016(3)	0	0.0070(4)
M(4)	0	0.27729(3)	½	0.0150(3)	0.0104(3)	0.0146(3)	0	0.0089(2)	0	0.0125(3)
A(2)	0	0.4872(3)	0							0.0171(9)
A(m)	0.5361(5)	0	0.0853(11)							0.0171(9)
O(1)	0.11069(11)	0.08592(6)	0.21804(19)	0.0057(4)	0.0077(4)	0.0067(4)	−0.0003(3)	0.0011(3)	−0.0007(3)	0.0068(2)
O(2)	0.11870(11)	0.16987(6)	0.7265(2)	0.0057(4)	0.0095(4)	0.0078(4)	−0.0007(3)	0.0014(3)	−0.0006(3)	0.0078(2)
O(3)	0.10657(16)	0	0.7140(3)	0.0085(6)	0.0092(6)	0.0088(6)	0	0.0024(4)	0	0.0088(4)
O(4)	0.36283(12)	0.24841(7)	0.7937(2)	0.0116(4)	0.0084(4)	0.0104(4)	−0.0007(3)	0.0032(3)	−0.0038(3)	0.0101(2)
O(5)	0.34638(12)	0.13146(7)	0.09485(19)	0.0080(4)	0.0147(5)	0.0085(4)	0.0046(3)	0.0020(3)	0.0005(3)	0.0104(2)
O(6)	0.34224(12)	0.11621(7)	0.59399(19)	0.0081(4)	0.0126(4)	0.0083(4)	−0.0034(3)	0.0014(3)	0.0007(3)	0.0099(2)
O(7)	0.33707(17)	0	0.2900(3)	0.0095(6)	0.0065(6)	0.0173(7)	0	0.0019(5)	0	0.0114(3)
					AM5					
T(1)	0.28004(4)	0.08506(2)	0.30208(8)	0.0079(2)	0.0082(2)	0.0080(2)	−0.00019(12)	0.00163(14)	−0.00052(12)	0.00817(14)
T(2)	0.28950(4)	0.17281(2)	0.81057(7)	0.0070(2)	0.0075(2)	0.0065(2)	0.00028(12)	0.00183(14)	−0.00039(12)	0.00700(14)
M(1)	0	0.08896(4)	½	0.0085(3)	0.0080(3)	0.0067(3)	0	0.0025(2)	0	0.0077(2)
M(2)	0	0.17628(4)	0	0.0073(3)	0.0071(3)	0.0070(3)	0	0.0024(2)	0	0.0071(2)
M(3)	0	0	0	0.0076(5)	0.0078(5)	0.0062(4)	0	0.0019(3)	0	0.0072(3)
M(4)	0	0.27899(2)	½	0.0140(2)	0.0114(2)	0.0123(2)	0	0.00664(16)	0	0.01205(16)
A(2)	0	0.4764(4)	0							0.032(2)
A(m)	0.5382(10)	0	0.086(2)							0.032(2)
O(1)	0.10771(11)	0.08616(6)	0.2179(2)	0.0082(4)	0.0128(5)	0.0083(4)	−0.0006(3)	0.0019(3)	−0.0016(3)	0.0099(2)
O(2)	0.11933(11)	0.17190(6)	0.7295(2)	0.0067(4)	0.0105(4)	0.0092(4)	0.0004(3)	0.0017(3)	0.0006(3)	0.0089(2)
O(3)	0.10702(15)	0	0.7162(3)	0.0092(6)	0.0096(6)	0.0109(6)	0	0.0024(5)	0	0.0100(4)
O(4)	0.36546(12)	0.24983(6)	0.7887(2)	0.0132(5)	0.0096(4)	0.0120(4)	−0.0001(3)	0.0046(3)	−0.0031(3)	0.0114(2)
O(5)	0.34947(11)	0.13886(7)	0.1095(2)	0.0104(4)	0.0162(5)	0.0096(4)	0.0046(3)	0.0011(3)	−0.0001(3)	0.0124(2)
O(6)	0.34461(11)	0.11554(7)	0.6093(2)	0.0100(4)	0.0138(5)	0.0128(4)	−0.0042(3)	0.0031(3)	0.0006(3)	0.0122(2)
O(7)	0.34175(17)	0	0.2774(3)	0.0108(6)	0.0123(7)	0.0176(7)	0	0.0034(5)	0	0.0137(3)

TABLE 3. SELECTED INTERATOMIC DISTANCES (Å) FOR GEM-QUALITY AMPHIBOLES FROM AFGHANISTAN

| Sample	AM4	AM5
$T(1)$–O(1)	1.5861(14)	1.6440(15)
$T(1)$–O(5)	1.6381(13)	1.6755(14)
$T(1)$–O(6)	1.6317(14)	1.6729(16)
$T(1)$–O(7)	1.6363(11)	1.6641(12)
$<T(1)$–O$>$	1.6231(13)	1.6641(14)
$T(2)$–O(2)	1.5930(14)	1.6235(15)
$T(2)$–O(4)	1.5753(14)	1.5937(14)
$T(2)$–O(5)a	1.6655(14)	1.6516(15)
$T(2)$–O(6)	1.6869(13)	1.6708(14)
$<T(2)$–O$>$	1.6302(14)	1.6349(15)
$M(1)$–O(1)	2.0672(14)	2.0467(15)
$M(1)$–O(1)d	2.0672(14)	2.0467(15)
$M(1)$–O(2)	2.0420(14)	2.0822(14)
$M(1)$–O(2)d	2.0421(14)	2.0822(14)
$M(1)$–O(3)	2.0765(13)	2.0854(14)
$M(1)$–O(3)e	2.0765(13)	2.0854(14)
$<M(1)$–O$>$	2.0619(14)	2.0714(14)
$M(2)$–O(1)	2.1533(15)	2.1074(15)
$M(2)$–O(1)f	2.1533(15)	2.1075(15)
$M(2)$–O(2)b ×2	2.0921(14)	2.0791(15)
$M(2)$–O(4)c ×2	1.9866(14)	2.0004(14)
$<M(2)$–O$>$	2.0773(14)	2.0623(15)
$M(3)$–O(1)g ×3	2.0579(13)	2.0532(14)
$M(3)$–O(1)	2.0580(13)	2.0532(14)
$M(3)$–O(3)b ×2	2.0561(17)	2.0488(18)
$<M(3)$–O$>$	2.0573(14)	2.0517(15)
$M(4)$–O(2)	2.4043(15)	2.4122(16)
$M(4)$–O(2)d	2.4044(15)	2.4122(16)
$M(4)$–O(4)c ×2	2.3572(15)	2.3294(16)
$M(4)$–O(5)c ×2	2.8043(16)	2.6536(17)
$M(4)$–O(6)c ×2	2.5916(16)	2.5987(17)
$<M(4)$–O$>$	2.5394(16)	2.4985(17)
$A(m)$–O(5)h ×2	2.896(3)	3.021(4)
$A(m)$–O(6)i ×2	2.756(4)	2.698(8)
$A(m)$–O(7)	2.476(4)	2.414(6)
$A(m)$–O(7)h	2.609(4)	2.506(7)
$<A(m)$–O$>$	2.732(4)	2.726(6)
$A(2)$–O(5)j ×2	2.733(4)	2.701(6)
$A(2)$–O(6)c ×2	2.953(3)	2.773(5)
$A(2)$–O(7)j ×2	2.505(2)	2.445(2)
$<A(2)$–O$>$	2.730(3)	2.640(5)

a: x, y, z + 1; b: x, y, z − 1; c: −x + 1/2, −y + 1/2, −z + 1; d: −x, y, −z + 1; e: −x, −y, −z + 1; f: −x, y, −z; g: −x, −y, −z; h: −x + 1, −y, −z; i: −x + 1, −y, −z + 1; j: −x + 1/2, −y + 1/2, −z

TABLE 4. CHEMICAL COMPOSITION (wt.%) AND UNIT FORMULA (*apfu*) OF GEM AMPHIBOLES FROM AFGHANISTAN

Sample	AM4	AM5
SiO_2	56.44	47.42
Al_2O_3	1.96	11.96
TiO_2	0.12	0.11
V_2O_3	0.01	0.02
Cr_2O_3	0.01	0.01
FeO	0.09	0.22
ZnO	0.01	0.01
MgO	23.94	21.71
CaO	7.73	12.03
Na_2O	5.75	4.06
K_2O	1.93	0.53
F	1.35	1.60
MnO	0.03	0.01
Cl	0.01	0.01
H_2O	1.54	1.40
O=F	−0.57	−0.67
Total	100.35	100.42
Si	7.75	6.57
Al	0.25	1.43
ΣT	8.00	8.00
Al^{3+}	0.07	0.52
Ti^{4+}	0.01	0.01
V^{3+}	0.00	0.00
Cr^{2+}	0.00	0.00
Fe^{2+}	0.01	0.03
Mg^{2+}	4.90	4.49
ΣC	4.99	5.05
Ca^{2+}	1.14	1.79
Na^+	0.86	0.21
ΣB	2.00	2.00
K^+	0.34	0.09
Na^+	0.67	0.88
ΣA	1.01	0.97
OH	1.41	1.30
F	0.59	0.70
ΣO(3)	1.99	2.00

SITE-POPULATIONS

The $C2/m$ amphibole structure is shown in Figure 1, and detailed summaries of previous work on amphibole crystal chemistry are given by Hawthorne (1981, 1983), Hawthorne & Oberti (2007), and Oberti *et al.* (2007). Refined site-scattering values (Hawthorne *et al.* 1995) and assigned site populations for AM4 and AM5 are given in Table 5.
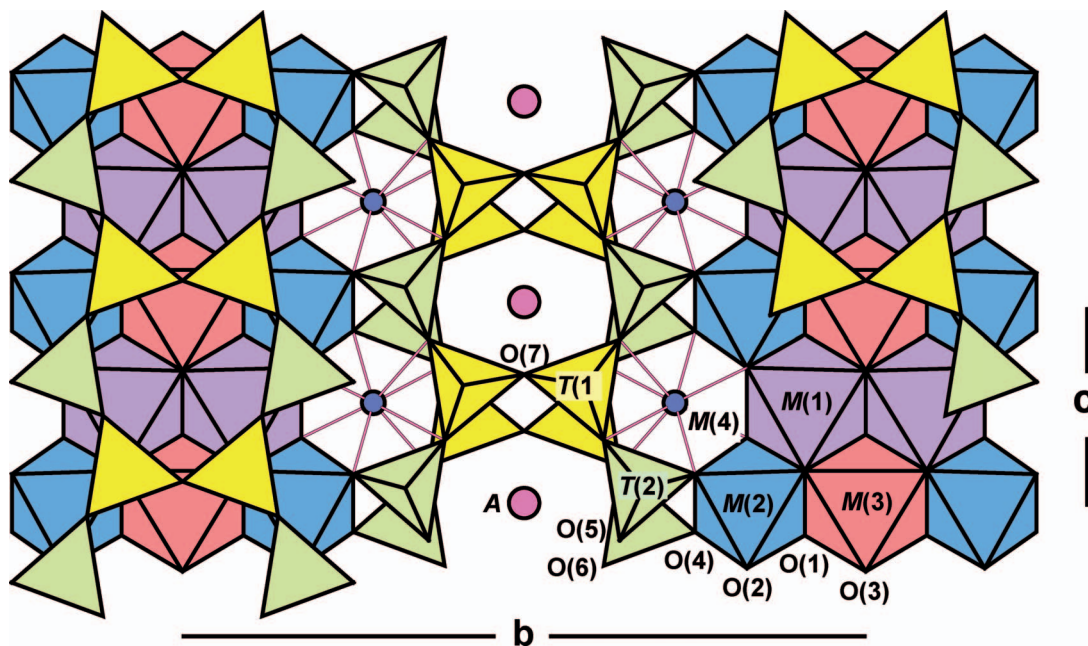
FIG. 1. The monoclinic *C2/m* amphibole structure viewed along [001].

TABLE 5. REFINED SITE-SCATTERING VALUES (*epfu*) AND ASSIGNED SITE-POPULATIONS (*apfu*)

Site	AM#	Assigned site population	Σ	refined s.s. values	calc. s.s. values	<bl> (Å)
T(1)	4	3.83 Si + 0.17 Al	4.00	–	–	1.623
	5	2.62 Si + 1.38 Al	4.00	–	–	1.664
T(2)	4	3.92 Si + 0.08 Al	4.00	–	–	1.630
	5	3.86 Si + 0.14 Al	4.00	–	–	1.635
M(1)	4	1.99 Mg + 0.01 Fe^{2+}	2.00	24.43(12)	24.14	2.062
	5	1.98 Mg + 0.02 Fe^{2+}	2.00	24.34(11)	24.28	2.071
M(2)	4	1.92 Mg + 0.07 Al + 0.01 Ti^{4+}	2.00	24.36(12)	24.17	2.077
	5	1.71 Mg + 0.28 Al + 0.01 Ti^{4+}	2.00	24.62(11)	24.38	2.062
M(3)	4	1.00 Mg	1.00	12.13(8)	12.00	2.057
	5	0.76 Mg + 0.24 Al	1.00	12.19(8)	12.24	2.052
M(4)	4	1.12 Ca + 0.88 Na	2.00	32.12(12)	32.08	2.539
	5	1.82 Ca + 0.18 Na	2.00	38.72(11)	38.38	2.498
A(m)	4	0.04 Na + 0.33 K	0.37	5.88(11)	6.71	2.732
	5	0.35 Na + 0.09 K	0.44	5.15(3)	5.56	2.726
A(2)	4	0.63 Na	0.63	6.26(10)	6.93	2.730
	5	0.56 Na	0.56	6.71(3)	6.16	2.640

The T sites

AM4 contains 0.25 [4]Al *apfu* and AM5 contains 1.43 [4]Al *apfu*, and the grand <*T*–O> distances of Table 3 are in accord with these values. Using the equation of Hawthorne & Oberti (2007) for predicting the grand <*T*–O> distance in amphiboles from the [4]Al content, the following distances were calculated: 1.629 and 1.648 Å compared to the experimental values of 1.627 and 1.650 Å for AM4 and AM5, respectively (Table 3). Consider next the Al occupancies of the *T*(1) and *T*(2) sites separately. As shown by

TABLE 6. BAND POSITIONS, INTENSITIES, AND ASSOCIATED LOCAL ARRANGEMENTS
FOR GEM AMPHIBOLES FROM AFGHANISTAN

Band	Center (cm^{-1})	Obs. intensity	Calc. intensity	Local arrangement
		AM4		
E	3730.10	0.42	0.50	(1) MgMgMg–OH–Na–OH:SiSi
F	3711.96	0.34	0.30	(2) MgMgMg–OH–Na–F:SiSi
B	3697.96	0.15	0.13	(4) MgMgMg–OH–Na–F:SiAl
G	3674.38	0.09	0.07	(7) MgMgMg–OH–□–OH:SiSi
		AM5		
A	3713.35	0.43	0.47	(3) MgMgMg–OH–Na–OH:SiAl
B	3692.58	0.20	0.16	(4) MgMgMg–OH–Na–F:SiAl
C	3681.62	0.21	0.27	(5) MgMgAl–OH–Na–OH:SiAl
D	3664.54	0.16	0.10	(6) MgMgAl–OH–Na–F:SiAl

Hawthorne & Oberti (2007, Fig. 17), there is no relation between individual $<T–O>$ distances and [4]Al where [4]Al $\leq$ 0.50 *apfu* and hence we have no reliable way to assign individual *T*-site populations in AM4. This is not the case for AM5. Using the site-specific equations of Hawthorne & Oberti (2007, Table 6), the following [4]Al site-populations are derived: $^{T(1)}$Al = 1.38, $^{T(2)}$Al = 0.14 *apfu*, the sum of which agrees closely with the experimental value of ^{T}Al = 1.43 *apfu* (Table 4).

The M(1,2,3) sites

The compositions of the C-group are dominated by Mg (4.49–4.90 *apfu*) and Al (0.07–0.52 *apfu*) in both AM4 and AM5 (Table 4). Semet (1973) showed by infrared spectroscopy that [6]M^{3+} cations disorder over the *M*(2) and *M*(1) and/or *M*(3) sites in Mg-rich synthetic amphiboles, and Raudsepp *et al*. (1987a, b, 1991) and Welch & Knight (1999) showed that this disorder occurs over the *M*(2) and *M*(3) sites. This pattern of order for [6]Al was confirmed in natural Mg-rich amphiboles by Oberti *et al*. (1995a), Tait *et al*. (2001), Heavysege *et al*. (2015), and Day *et al*. (2018). The absence of Al at the *M*(1) site and the excess scattering over that expected for complete occupancy by Mg allows us to assign Fe to the *M*(1) site (Table 5). We assign Ti to the *M*(2) site. The X-ray scattering factors of Mg (*Z* = 12) and Al (*Z* = 13) are very close, and therefore mean bond-lengths must be used to assign [6]Al and [6]Mg, as the sizes of [6]Mg (r = 0.72 Å) and [6]Al (r = 0.535 Å) differ significantly (Shannon 1976). Using the equations relating $<M(2)–O>$ and $<M(3)–O>$ distances to constituent cation and anion radii and to other stereochemical aspects of the adjacent sites (Hawthorne & Oberti 2007), [6]Al and [6]Mg were assigned to *M*(2) and *M*(3) such that there is an equally good fit between the observed and

calculated $<M(2)–O>$ and $<M(3)–O>$ values (Table 5).

The M(4) site

The unit formulae (Table 4) indicate that the *M*(4) site is occupied by Ca and Na, in accord with the refined site-scattering values. Thus the site populations were assigned directly from the formulae in Table 4.

The A site

Following Hawthorne & Grundy (1972, 1973a, b) and Hawthorne *et al*. (1996b), Na was assigned to the *A*(2) site and (Na + K) was assigned to the *A*(m) site (Table 5). The refined site-scattering at the *A* sites in AM4 and AM5 (Table 5) are 12.14 and 11.86 *epfu*, respectively, whereas the corresponding values calculated from the site-populations of Table 5 are 13.64 and 11.72 *epfu*. There is close agreement for AM5, but for AM4 there is a difference of 1.50 *epfu*. This issue will be important to a later discussion on the principal OH-stretching region in the infrared spectrum of AM4.

INFRARED SPECTROSCOPY

FTIR spectra were fit to Gaussian curves with similar width (full-width-at-half-maximum) using the program FITYK V0.9.8; the numerical details of each of the fitted spectra are given in Table 6. Fitted FTIR spectra for AM4 and AM5 in the principal (OH)-stretching region are shown in Figure 2a and Figure 2b, respectively.

SHORT-RANGE ARRANGEMENTS

Short-range arrangements are common in amphiboles and may be characterized using a combination of infrared and Raman spectroscopy (*e.g*., Hawthorne *et al*. 1996a) and local bond-valence requirements
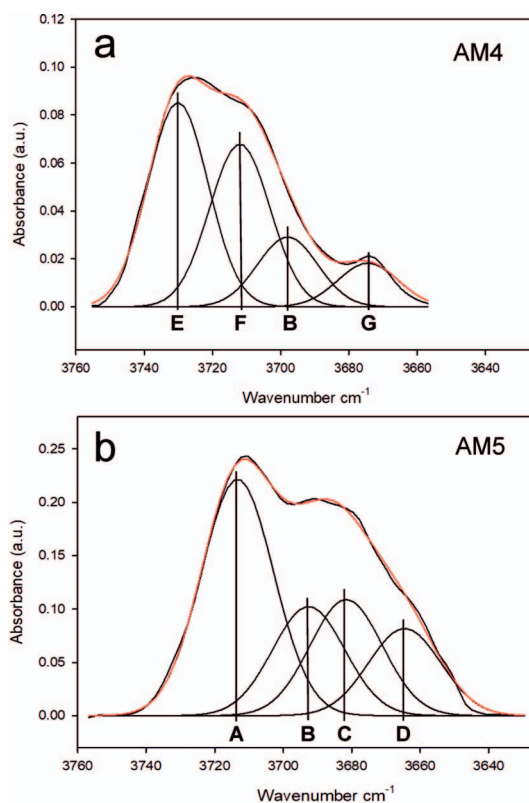
Fig. 2. The spectra in the principal (OH)-stretching region of (a) AM4 and (b) AM5. Black curves represent the observed spectra and red curves represent the resultant fitted line.

(Hawthorne 1997). The principal OH-stretching frequency is affected by both nearest-neighbor (NN) and next-nearest-neighbor (NNN) ions that interact with the locally associated $^{O(3)}$(OH) group (e.g., Hawthorne 2016, Hawthorne et al. 1997, 2000, Della Ventura et al. 1999, 2001, 2003, Robert et al. 1999, 2000, Hawthorne & Della Ventura 2007, Leissner et al. 2015, Della Ventura, 2017), and local arrangements can be assigned from a combination of spectroscopic, crystallographic, and chemical-analytical work.

THE CONFIGURATION SYMBOL AND POSSIBLE LOCAL ARRANGEMENTS

The arrangement of crystallographic sites around the O(3) site in the amphibole structure is called the "configuration symbol", and may be written as $M(1)M(1)M(3)$–O(3)–A:$T(1)T(1)$–$M(2)M(2)M(3)$–$M(2)M(2)$ (Hawthorne et al. 2005). The number of sites included in this symbol may vary according to the chemical composition of the amphibole and its spectral

complexity. Assignment of different ions to the sites in the configuration symbol gives rise to possible local arrangements that may correspond to bands in the vibrational spectrum. Differences in NNN cation occupancies produce minor splitting in the major bands of pargasite (Della Ventura et al. 1999). However, Robert et al. (2000) successfully fitted the spectra of pargasite–fluoro-pargasite solid-solutions using single composite bands; we have done likewise here for AM5. Such band-splitting will not occur in the spectrum of AM4 as there is no disorder at the NNN cation-sites (Tables 4 and 5).

In order to incorporate the NNN effect of $^{O(3)}$F across an occupied A-site, we expand the configuration symbol to be $M(1)M(1)M(3)$–O(3)–A–O(3):$T(1)T(1)$ (Day et al. 2018), where we have omitted NNN M-sites because either they have no effect (AM4) or we are fitting composite bands that average their effects (AM5). The following arrangements of $^{O(3)}$(OH)/F about the A site are possible: $M(1)M(1)M(3)$–OH–A–OH:$T(1)T(1)$; $M(1)M(1)M(3)$–OH–A–F:$T(1)T(1)$; $M(1)M(1)M(3)$–F–A–OH:$T(1)T(1)$; $M(1)M(1)M(3)$–F–A–F:$T(1)T(1)$; the last arrangement has no expression in the infrared.

Constraints on composition

(1) A-group cations completely occupy the A site in both AM4 and AM5 and local arrangements must involve only A = Na* (Na* = Na + K) (Table 4). Although the compositional data for AM4 indicates a fully occupied A-site, slight differences between the refined and calculated site-scattering values (epfu) (Table 5) suggest the possibility of a small vacancy component at the A sites.

(2) As noted above, for amphiboles where Mg is dominant at the $M(1,2,3)$ sites, trivalent C-group cations are partly disordered over the $M(2)$ and $M(3)$ sites. Here, the $M(3)$ site-populations from Table 5 are used to calculate the relative amounts of the local arrangements at $M(1)M(1)M(3)$ as follows: MgMgMg:MgMgAl = $^{M(3)}$Mg*:$^{M(3)}$Al (Mg* = Mg + Fe^{2+}) (Day et al. 2018). In both these amphiboles, $^{M(3)}$Mg* >> $^{M(3)}$Al (Table 5) and hence local arrangements involving MgMgAl are less common than their MgMgMg analogues. In AM4 richterite, the $M(3)$ site is completely occupied by Mg (with negligible Fe^{2+} content) (Table 5) and therefore all $M(1)M(1)M(3)$ arrangements correspond to MgMgMg.

(3) The $T(1)T(1)$ arrangement can be rewritten as $T(1)$–O(7)–$T(1)$ as T(1) cations link to one another via O(7). The $T(1)$–O(7)–$T(1)$ arrangements are strongly affected by the amount of $^{[4]}$Al in the structure. Due to a bond-valence deficiency at the

O(7) site, the arrangement $^{T(1)}$Al–O(7)–$^{T(1)}$Al cannot occur unless Ca occupies the A site. As the A sites in AM4 and AM5 are fully occupied by Na + K, $^{T(1)}$Al–O(7)–$^{T(1)}$Al arrangements are not possible and the T-site populations (Table 5) may be used to calculate the frequencies of occurrence of $T(1)T(1)$ arrangements as follows: $^{T(1)}$Al–O(7)–$^{T(1)}$Si = $^{T(1)}$Al/2 and $^{T(1)}$Si–O(7)–$^{T(1)}$Si = 1 – $^{T(1)}$Al/2 (Day et al. 2018).

(4) In AM4 and AM5, there is only minor occupancy of the $M(1,2,3)$ sites by divalent cations other than Mg. The amount of Fe^{2+} ranges from 0.01–0.02 apfu and therefore the $M(1)M(1)M(3)$ = MgMgFe arrangements can be ignored.

(5) $M(1)M(1)M(3)$ = MgMgAl arrangements should be preferentially associated with the arrangement $T(1)T(1)$ = SiAl, as this arrangement would result in a slight bond-valence deficiency at the O(7) site compared to the arrangement $T(1)T(1)$ = SiSi (Heavysege et al. 2015). Thus the local arrangement $M(1)M(1)M(3)$–O(3)–A–O(3):$T(1)T(1)$ = MgMgMg–OH–Na*–OH:SiSi will be dominant in AM4 in which there is minor $^{[4]}$Al. Conversely, we do not expect MgMgMg–OH–Na*–OH:SiSi arrangements in AM5 because of the abundant $^{T(1)}$Al in the structure (Table 5).

The nearest-neighbor effect of F

Local arrangements involving the $M(3)$ site can be written as O(3)–$M(3)$–O(3), as each $M(3)$ site is linked to two symmetrically equivalent O(3) sites (Hawthorne et al. 2005). For amphiboles in which the O(3) site is occupied by (OH) and F, the following local arrangements are possible: (OH)–$M(3)$–(OH); (OH)–$M(3)$–F [= F–$M(3)$–(OH)]; and F–$M(3)$–F; and give rise to two, one, and zero absorption events in the infrared, respectively. It follows that the proportion of absorption events to null-absorption events is equal to the (OH):F ratio regardless of any SR–OD effects that $M(3)$ cations may exert on F (Heavysege et al. 2015).

For amphiboles in which the O(3) site is occupied by F, there is no disorder of trivalent cations over $M(2)$ and $M(3)$ (Raudsepp et al. 1987b, Oberti et al. 1995b, 1998, Della Ventura et al. 2014). It follows that in amphiboles such as AM4 and AM5, in which the O(3) site is occupied by F and (OH), F is partly to strongly short-range ordered with respect to the arrangement $M(1)M(1)M(3)$ = MgMgMg as opposed to the arrangement $M(1)M(1)M(3)$ = MgMgAl. This ordering is only operative in amphiboles containing $^{M(3)}$Al (such as AM5). Inspection of Table 4 shows that $^{O(3)}$F > $^{M(3)}$Al in AM5, suggesting that F must also be partly associated with the arrangement $M(1)M(1)M(3)$ = MgMgAl. For both AM4 and AM5, $^{T(1)}$Al/2 > $^{M(3)}$Al which is in

accord with the relative amounts of the $T(1)T(1)$ arrangements: SiSi:SiAl: = (1 – $^{T(1)}$Al/2) : $^{T(1)}$Al/2 proposed above in (3) (Table 5). In AM4, the local arrangement MgMgMg–OH–Na–OH–SiSi gives rise to a band at ~3730 cm^{-1} as the number of arrangements $T(1)T(1)$ = Si Si = 1 – $^{T(1)}$Al/2 is more than the amount of F (Della Ventura et al. 1999, Hawthorne 2016). In AM5, an analogous band at 3730–3740 cm^{-1} is not observed, as the number of arrangements $T(1)T(1)$ = Si Si = 1 – $^{T(1)}$Al/2 is always less than the amount of F, and therefore all local arrangements MgMgMg–X–Na:SiSi will have X = F and no expression in the infrared. Della Ventura et al. (2014) reported a similar absence of a band at 3730–3740 cm^{-1} in the spectra of fluoro-edenite and fluoro-pargasite.

The next-nearest-neighbor effect of F

In the infrared spectra of tremolite and fluoro-tremolite, there is a single (OH)-stretching band at ~3674 cm^{-1} (Della Ventura et al. 2003, Hawthorne et al. 1997, 2000). The position of this band does not change significantly with increasing F content as there is no coupling between adjacent $^{O(3)}$(OH,F) across the vacant A site; this is known as "one-mode behavior" (Chang & Mitra 1968, Hawthorne & Della Ventura 2007). For amphiboles in which there are local arrangements with the A site occupied and both neighboring O(3) sites occupied by (OH), there will be repulsion between both H^+ ions and the A-site cation, which forces the A-site cation to occupy a more central position (Hawthorne et al. 2005) and causes the principal (OH)-stretching band to occur at higher frequency compared to an arrangement where the A site is vacant. Where one O(3) site across the A cavity is occupied by F, no such repulsion occurs and the A-group cation moves away from the (OH) group towards the other O(3) site, decreasing the repulsion between H^+ and the A-site cation, whereupon the OH–^{A}Na–F arrangement will absorb at a relatively lower wavenumber. This is known as "two-mode behavior" (Chang & Mitra 1968). It follows that in amphiboles with $^{O(3)}$(OH,F) and an occupied A site (such as AM4 and AM5), the local arrangements OH–^{A}Na–OH, OH–^{A}Na–F, and F–^{A}Na–F will occur. The frequency of such arrangements may be calculated using the F content of each sample (Heavysege et al. 2015) where x = F/(F + OH).

$$\text{OH}-^A\text{Na}-\text{OH:} \quad (1-x)^2/\left(1-x+x^2\right)$$

$$\text{OH}-^A\text{Na}-\text{F:} \quad x(1-x)^2/\left(1-x+x^2\right)$$

$$\text{F}-^A\text{Na}-\text{F:} \quad x^2/\left(1-x+x^2\right)$$

The relative amounts of these local arrangements involving A = Na* (Na* = Na + K) and $^{O(3)}$(OH,F) may be calculated from the expressions listed above. Bands that correspond to arrangements involving F–^{A}Na–F will not be visible in the infrared.

As discussed in (2), we expect the NN configuration of AM5 to have two principal arrangements, MgMgMg and MgMgAl. Moreover, we expect all $T(1)T(1)$ = SiAl as $T(1)T(1)$ = SiSi = $(1 - ^{T(1)}Al/2)$ is less than the amount of F in AM5 (Table 4). The arrangements MgMgMg–OH–Na–OH:SiAl and MgMgAl–OH–Na–OH:SiAl are expected to produce bands at 3710–3720 cm^{-1} and 3677–3687 cm^{-1}, respectively (Day *et al.* 2018). It follows that each of these $M(1)M(1)M(3)$ arrangements should have an F-shifted equivalent, MgMgMg–OH–Na–F:SiAl and MgMgAl–OH–Na–F:SiAl (Table 6). Such arrangements should give rise to bands at 3700–3690 cm^{-1} and 3667–3657 cm^{-1}, respectively, as $^{M(1,3)}$Mg substituted by $^{M(1,3)}$Al and $^{O(3)}$OH substituted by $^{O(3)}$F results in a relative band-displacement of ~33 cm^{-1} and ~15–20 cm^{-1}, respectively (Robert *et al.* 1999, 2000, Della Ventura *et al.* 1999). In AM4, we expect only one principal arrangement, MgMgMg, and the arrangement $T(1)T(1)$ = SiSi should occur more frequently than $T(1)T(1)$ = SiAl, as $T(1)T(1)$ = Si Si = $(1 - ^{T(1)}Al/2)$ is greater than the amount of F in AM4 (Table 4) [constraints (2) and (3)]. Consequently, the arrangement MgMgMg–OH–Na–OH:SiSi, which is expected to produce a band at ~3730 cm^{-1}, will have an F-shifted equivalent: MgMgMg–OH–Na–F:SiSi. Such an arrangement should produce a band at ~3710–3715 cm^{-1} (Robert *et al.* 1999, 2000). Unfortunately, we also expect a band at ~3710 cm^{-1} due to the arrangement MgMgMg–OH–Na–OH:SiAl, as $^{T(1)}$Si substituted by $^{T(1)}$Al results in a band displacement of ~20 cm^{-1}, similar to the band displacement effect of $^{O(3)}$OH substituted by $^{O(3)}$F (~15–20 cm^{-1}) (Della Ventura *et al.* 1999). Any band intensity corresponding to this arrangement in AM4 will likely be masked by the band from the arrangement MgMgMg–OH–Na–F:SiSi, as the amount of $^{T(1)}$Al (0.17 *apfu*) is much less than the amount of $^{O(3)}$F (0.59 *apfu*). We also expect another low intensity band at ~3690–3695 cm^{-1} due to the arrangement MgMgMg–OH–Na–F:SiAl.

The resulting arrangements are numbered as follows: (1) MgMgMg–OH–Na–OH:SiSi; (2) MgMgMg–OH–Na–F:SiSi; (3) MgMgMg–OH–Na–OH:SiAl; (4) MgMgMg–OH–Na–F:SiAl; (5) MgMgAl–OH–Na–OH:SiAl; (6) MgMgAl–OH–Na–F:SiAl; (7) MgMgMg–OH–□–OH:SiSi (Table 6).

Description and Interpretation of the Spectra

AM4

The spectrum of AM4 was fitted using four peaks (Fig. 2a); however, the assignment of such peaks differs in AM4 and AM5. Hence the labels attached to the peaks in each spectrum are the same only where the assignment to a specific local arrangement is the same; otherwise the labels are different (Fig. 2a, b). Following previous work (*e.g.*, Robert *et al.* 1989, 1999, Della Ventura *et al.* 1998a, 1999, Hawthorne *et al.* 1997), these peaks correspond to the local arrangements: (1) MgMgMg–OH–Na–OH:SiSi; (2) MgMgMg–OH–Na–F:SiSi; (4) MgMgMg–OH–Na–F:SiAl; and (7) MgMgMg–OH–□–OH:SiSi (Table 6). Each of the four bands is located within or close to the ideal frequency ranges calculated above. The two strongest bands (E and F) in richterite and fluoro-richterite occur at ~3730 and ~3711 cm^{-1} and are due to arrangements (1) and (2) (Table 6) (Della Ventura *et al.* 1996a, 1998a, 1999, Hawthorne *et al.* 1997, 2005, Hawthorne & Della Ventura 2007). There is a small amount of $^{T(1)}$Al in AM4 and this will give rise to the local arrangement (3) MgMgMg–OH–Na–OH:SiAl which will produce a peak at ~3710 cm^{-1} that overlaps with band F. However, the amount of $^{T(1)}$Al (0.17 *apfu*) in AM4 is minimal and therefore the contribution from this arrangement is small. Band F is therefore dominated by absorption from arrangement (2) and the observed and calculated intensities for band F are in close agreement (Table 6). Band B (Table 6) is located at ~3698 cm^{-1} and has been assigned the local arrangement (4) MgMgMg–OH–Na–F:SiAl. A band at a similar location (~3694 cm^{-1}) has been reported in the spectra of amphiboles along the richterite–pargasite join and in potassium-fluoro-richterite (Della Ventura *et al.* 1998a).

Band G at ~3674 cm^{-1} has been interpreted in previous work (Rowbotham & Farmer 1974, Della Ventura *et al.* 1998a, Hawthorne *et al.* 1997, 2006) as a "tremolite-like" component, corresponding to the (7) MgMgMg–OH–□–OH:SiSi arrangement. The chemical formula (Table 4) shows that the A-group cations completely fill the *A*-sites and for this reason are not compatible with the presence of a tremolite-like component (*i.e.*, vacancy at the A group). However, discrepancy between the refined and calculated site-scattering values at $A(2)$ and $A(m)$ (1.50 *epfu*) indicate significant *A*-site vacancy (0.15 □ *pfu*) in accordance with the presence of band G in the infrared spectrum of AM4.

AM5

The spectrum of AM5 (Fig. 2b) was fitted using four peaks. Following Day *et al.* (2018), these peaks

were then assigned to the local arrangements: (3) MgMgMg–OH–Na–OH:SiAl; (4) MgMgMg–OH–Na–F:SiAl; (5) MgMgAl–OH–Na–OH:SiAl; and (6) MgMgAl–OH–Na–F:SiAl (Table 6). The intensities of these bands are in reasonable accord with the calculated amounts of the local arrangements, and the absorption frequencies of the bands are similar to those observed in the spectra of similar pargasite and fluoro-pargasite amphiboles (Day *et al.* 2018).

Summary

In both amphiboles, [4]Al occupies both $T(1)$ and $T(2)$ but is strongly ordered at $T(1)$ in pargasite. $M(1,2,3)$ are occupied by predominately [6]Mg, and [6]Al is partly disordered over $M(2)$ and $M(3)$ in pargasite. Minor [6]Fe^{2+} occurs at $M(1)$ and other tetravalent cations, particularly [6]Ti^{4+}, are weakly ordered at $M(2)$. ^{A}K occurs at the $A(m)$ site and ^{A}Na occupies both the $A(m)$ and $A(2)$ sites. The infrared spectrum of each amphibole was fitted to four constituent bands. In AM4, bands E (at ∼3730 cm^{-1}), F (at ∼3712 cm^{-1}), B (at ∼3698 cm^{-1}), and G (at ∼3674 cm^{-1}) correspond to the local arrangements (1) MgMgMg–OH–Na–OH:SiSi, (2) MgMgMg–OH–Na–F:SiSi, (4) MgMgMg–OH–Na–F:SiAl, and (7) MgMgMg–OH–□–OH:SiSi, respectively. In AM5, bands A (at ∼3713 cm^{-1}), B (at ∼3693 cm^{-1}), C (at ∼3682 cm^{-1}), and D (at ∼3665 cm^{-1}) correspond to the local arrangements (3) MgMgMg–OH–Na–OH:SiAl, (4) MgMgMg–OH–Na–F:SiAl, (5) MgMgAl–OH–Na–OH:SiAl, and (6) MgMgAl–OH–Na–F:SiAl, respectively.

References

ABDU, Y.A. & HAWTHORNE, F.C. (2009) Crystal structure and Mössbauer spectroscopy of tschermakite from the ruby locality at Fiskenaesset, Greenland. *Canadian Mineralogist* **47**, 917–926.

CHANG, I.F. & MITRA, S.S. (1968) Application of a modified random-element-isodisplacement model to long-wave-length optic phonons of mixed crystals. *Physical Review* **172**, 924–933.

DAY, M.C., HAWTHORNE, F.C., SUSTA, U., DELLA VENTURA, G., & HARLOW, G.E. (2018) Gem amphiboles from Mogok, Myanmar: crystal-structure refinement, infrared spectroscopy and short-range order-disorder in gem pargasite and fluoro-pargasite. *Mineralogical Magazine*, 1–36; DOI: 10.1180/mgm.2018.149.

DELLA VENTURA, G. (2017) The analysis of asbestos minerals using vibrational spectroscopies (FTIR, Raman): crystal-chemistry, identification and environmental applications. *In* Mineral fibres: crystal chemistry, chemical-physical properties, biological interactions and toxicity (A. Gualtieri, ed.). *EMU Notes in Mineralogy* **18**, 135–169.

DELLA VENTURA, G., ROBERT, J.L., HAWTHORNE, F.C., & PROST, R. (1996a) Short-range disorder of Si and Ti in the tetrahedral double-chain unit of synthetic Ti-bearing potassium richterite. *American Mineralogist* **81**, 56–60.

DELLA VENTURA, G., ROBERT, J.L., & HAWTHORNE, F.C. (1996b) Infrared spectroscopy of synthetic (Ni,Mg,Co)-potassium-richterite. *Geochimica et Cosmochimica Acta* **5**, 55–63.

DELLA VENTURA, G., ROBERT, J.L., RAUDSEPP, M., HAWTHORNE, F.C., & WELCH, M. (1997) Site occupancies in synthetic monoclinic amphiboles: Rietveld structure-refinement and infrared spectroscopy of (nickel, magnesium, cobalt)-richterite. *American Mineralogist* **82**, 291–301.

DELLA VENTURA, G., ROBERT, J.L., & HAWTHORNE, F.C. (1998a) Characterization of OH-F short-range order in potassium-fluor-richterite by infrared spectroscopy in the OH-stretching region. *Canadian Mineralogist* **36**, 181–185.

DELLA VENTURA, G., ROBERT, J.L., HAWTHORNE, F.C., RAUDSEPP, M., & WELCH, M.D. (1998b) Contrasting patterns of [6]Al order in synthetic pargasite and Co-substituted pargasite. *Canadian Mineralogist* **36**, 1237–1244.

DELLA VENTURA, G., HAWTHORNE, F.C., ROBERT, J.L., DELBOVE, F., WELCH, M.D., & RAUDSEPP, M. (1999) Short-range order of cations in synthetic amphiboles along the richterite-pargasite join. *European Journal of Mineralogy* **11**, 79–94.

DELLA VENTURA, G., ROBERT, J.L., SERGENT, J., HAWTHORNE, F.C., & DELBOVE, F. (2001) Constraints on F vs. OH incorporation in synthetic [6]Al-bearing monoclinic amphiboles. *European Journal of Mineralogy* **13**, 841–847.

DELLA VENTURA, G., HAWTHORNE, F.C., ROBERT, J.L., & IEZZI, G. (2003) Synthesis and infrared spectroscopy of amphiboles along the tremolite-pargasite join. *European Journal of Mineralogy* **15**, 341–347.

Della Ventura, G., Bellatreccia, F., Cámara, F., & Oberti, R. (2014) Crystal-chemistry and short-range order of fluoroedenite and fluoro-pargasite: a combined X-ray diffraction and FTIR spectroscopic approach. *Mineralogical Magazine* **78**, 293–310.

Hawthorne, F.C. (1981) Crystal Chemistry of the Amphiboles. *Reviews in Mineralogy* **9A**, 1–102.

Hawthorne, F.C. (1983) The crystal chemistry of the amphiboles. *Canadian Mineralogist* **21**, 173–480.

Hawthorne, F.C. (1997) Short-range order in amphiboles: A bond valence approach. *Canadian Mineralogist* **35**, 201–216.

Hawthorne, F.C. (2016) Short-range atomic arrangements in minerals. I: The minerals of the amphibole, tourmaline and pyroxene supergroups. *European Journal of Mineralogy* **28**, 513–536.

Hawthorne, F.C. & Della Ventura, G. (2007) Short-range order in amphiboles. *Reviews in Mineralogy and Geochemistry* **67**, 173–222.

Hawthorne, F.C. & Grundy, H.D. (1972) Positional disorder in the *A*-site of clino-amphiboles. *Nature* **235**, 72.

Hawthorne, F.C. & Grundy, H.D. (1973a) The crystal chemistry of the amphiboles. I. Refinement of the crystal structure of ferrotschermakite. *Mineralogical Magazine* **39**, 36–48.

Hawthorne, F.C. & Grundy, H.D. (1973b) The crystal chemistry of the amphiboles. II. Refinement of the crystal structure of oxykaersutite. *Mineralogical Magazine* **39**, 390–400.

Hawthorne, F.C. & Oberti, R. (2007) Amphiboles: Crystal chemistry. *Reviews in Mineralogy and Geochemistry* **67**, 1–54.

Hawthorne, F.C., Ungaretti, L., & Oberti, R. (1995) Site-populations in minerals: terminology and presentation of results. *Canadian Mineralogist* **33**, 907–911.

Hawthorne, F.C., Della Ventura, G., & Robert, J.-L. (1996a) Short-range order of (Na,K) and Al in tremolite: An infrared study. *American Mineralogist* **81**, 782–784.

Hawthorne, F.C., Oberti, R., & Sardone, N. (1996) Sodium at the A site in clinoamphiboles: the effects of composition on patterns of order. *Canadian Mineralogist* **34**, 577–593.

Hawthorne, F.C., Della Ventura, G., Robert, J.L., Welch, M.D., Raudsepp, M., & Jenkins, D.M. (1997) A Rietveld and infrared study of synthetic amphiboles along the potassium-richterite-tremolite join. *American Mineralogist* **82**, 708–716.

Hawthorne, F.C., Welch, M.D., Della Ventura, G., Liu, S., Robert, J.L., & Jenkins, D.M. (2000) Short-range order in synthetic aluminous tremolites: An infrared and triple-quantum MAS NMR study. *American Mineralogist* **85**, 1716–1724.

Hawthorne, F.C., Della Ventura, G., Oberti, R., Robert, J.L., & Iezzi, G. (2005) Short-range order in minerals: Amphiboles. *Canadian Mineralogist* **43**, 1895–1920.

Hawthorne, F.C., Oberti, R., & Martin, R.F. (2006) Short-range order in amphiboles from the Bear Lake Diggings, Ontario. *Canadian Mineralogist* **44**, 1171–1179.

Heavysege, D., Abdu, Y.A., & Hawthorne, F.C. (2015) Long-range and short-range order in gem pargasite from Myanmar: Crystal-structure refinement and infrared spectroscopy. *Canadian Mineralogist* **53**, 497–510.

Leissner, L., Schlüter, J., Horn, I., & Mihailova, B. (2015) Exploring the potential of Raman spectroscopy for crystallochemical analyses of complex hydrous silicates: I. Amphiboles. *American Mineralogist* **100**, 2682–2694.

Najorka, J. & Gottschalk, M. (2003) Crystal chemistry of tremolite–tschermakite solid solutions. *Physics and Chemistry of Minerals* **30**, 108–124.

Oberti, R., Hawthorne, F.C., Ungaretti, L., & Cannillo, E. (1995a) [6]Al disorder in amphiboles from mantle peridotites. *Canadian Mineralogist* **33**, 867–878.

Oberti, R., Sardone, N., Hawthorne, F.C., Raudsepp, M., & Turnock, A.C. (1995b) Synthesis and crystal-structure refinement of synthetic fluor-pargasite. *Canadian Mineralogist* **33**, 25–31.

Oberti, R., Hawthorne, F.C., Cámara, F., & Raudsepp, M. (1998) Synthetic fluoro-amphiboles: site preferences of Al, Ga, Sc and inductive effects on mean bond-lengths of octahedra. *Canadian Mineralogist* **36**, 1245–1252.

Oberti, R., Hawthorne, F.C., Cannillo, E., & Cámara, F. (2007) Long-range order in amphiboles. *Reviews in Mineralogy and Geochemistry* **67**, 125–171.

Pouchou, J.L. & Pichoir, F. (1985) 'PAP' φ(ρZ) procedure for improved quantitative microanalysis. *In* Microbeam Analysis (J.T. Armstrong, ed.). San Francisco Press, San Francisco, California (104–106).

Raudsepp, M., Turnock, A.C., & Hawthorne, F.C. (1987a) Characterization of cation ordering in synthetic scandium-fluor-eckermannite, indium-fluor-eckermanite, and scandium-fluor-nybøite by Rietveld structure refinement. *American Mineralogist* **72**, 959–964.

Raudsepp, M., Turnock A.C., Hawthorne, F.C., Sherriff, B.L., & Hartman, J.S. (1987b) Characterization of synthetic pargasitic amphiboles $(NaCa_2Mg_4M^{3+}Si_6Al_2O_{22}(OH,F)_2; M^{3+} = Al,Cr,Ga,Sc,In)$ by infrared spectroscopy, Rietveld structure refinement, and ^{27}Al, ^{29}Si, and ^{19}F MAS NMR spectroscopy. *American Mineralogist* **72**, 580–593.

RAUDSEPP, M., TURNOCK, A.C., & HAWTHORNE, F.C. (1991) Amphiboles synthesis at low-pressure: what grows and what doesn't. *European Journal of Mineralogy* **3**, 983–1004.

ROBERT, J.-L., DELLA VENTURA, G., & THAUVIN, J.-L. (1989) The infrared OH-stretching region of synthetic richterites in the system $Na_2O–K_2O–CaO–MgO–SiO_2–H_2O–HF$. *European Journal of Mineralogy* **1**, 203–211.

ROBERT, J.L., DELLA VENTURA, G., & HAWTHORNE, F.C. (1999) Near-infrared study of short-range disorder of OH and F in monoclinic amphiboles. *American Mineralogist* **84**, 86–91.

ROBERT, J.-L., DELLA VENTURA, G., WELCH, M.D., & HAWTHORNE, F.C. (2000) The OH/F substitution in synthetic pargasite at 1.5 kbar, 850 °C. *American Mineralogist* **85**, 926–931.

ROWBOTHAM, G. & FARMER, V.C. (1974) The effect of the "A" site occupancy upon the hydroxyl stretching frequency in clinoamphiboles. *Contributions to Mineralogy and Petrology* **38**, 147–149.

SEMET, M.P. (1973) A crystal-chemical study of synthetic magnesiohastingsite. *American Mineralogist* **58**, 480–494.

SHANNON, R.D. (1976) Revised effective ionic radii and systematic studies of interatomic distances in halides and chalcogenides. *Acta Crystallographica* **A32**, 751–767.

SHELDRICK, G.M. (2008) A short history of *SHELX*. *Acta Crystallographica* **A64**, 112–122.

TAIT, K.T., HAWTHORNE, F.C., & DELLA VENTURA, G. (2001) Al-Mg disorder in a gem-quality pargasite from Baffin Island, Nunavut, Canada. *Canadian Mineralogist* **39**, 1725–1732.

WELCH, M.D. & KNIGHT, K.S. (1999) A neutron powder diffraction study of cation ordering in high-temperature synthetic amphiboles. *European Journal of Mineralogy* **11**, 321–331.